The Plant Cell, Vol. 21: 595–606, February 2009, www.plantcell.org

Arabidopsis Photorespiratory Serine Hydroxymethyltransferase Activity Requires the Mitochondrial Accumulation of Ferredoxin-Dependent Glutamate Synthase [W]

Aziz Jamai,[a] Patrice A. Salomé,[a,1] Stephen H. Schilling,[a,2] Andreas P.M. Weber,[b] and C. Robertson McClung[a,3]

[a] Department of Biological Sciences, Dartmouth College, Hanover, New Hampshire 03755
[b] Heinrich-Heine-Universität, Institut für Biochemie der Pflanzen, 40225 Düsseldorf, Germany

The dual affinity of ribulose-1,5-bisphosphate carboxylase/oxygenase for O_2 and CO_2 results in the net loss of fixed carbon and energy in a process termed photorespiration. The photorespiratory cycle is complex and occurs in three organelles, chloroplasts, peroxisomes, and mitochondria, which necessitates multiple steps to transport metabolic intermediates. Genetic analysis has identified a number of mutants exhibiting photorespiratory chlorosis at ambient CO_2, including several with defects in mitochondrial serine hydroxymethyltransferase (SHMT) activity. One class of mutants deficient in SHMT1 activity affects *SHM1*, which encodes the mitochondrial SHMT required for photorespiration. In this work, we describe a second class of SHMT1-deficient mutants defective in a distinct gene, *GLU1*, which encodes Ferredoxin-dependent Glutamate Synthase (Fd-GOGAT). Fd-GOGAT is a chloroplastic enzyme responsible for the reassimilation of photorespiratory ammonia as well as for primary nitrogen assimilation. We show that Fd-GOGAT is dual targeted to the mitochondria and the chloroplasts. In the mitochondria, Fd-GOGAT interacts physically with SHMT1, and this interaction is necessary for photorespiratory SHMT activity. The requirement of protein–protein interactions and complex formation for photorespiratory SHMT activity demonstrates more complicated regulation of this crucial high flux pathway than anticipated.

INTRODUCTION

Ribulose-1,5-bisphosphate carboxylase/oxygenase (Rubisco) initiates the Calvin (C_3) cycle with the carboxylation of ribulose 1,5 bisphosphate to yield two molecules of 3-phosphoglycerate (3PGA). However, the dual affinity of Rubisco for O_2 and CO_2 means that Rubisco also catalyzes the oxygenation of ribulose 1,5 bisphosphate to yield one molecule of 3PGA and one molecule of 2-phosphoglycolate (2PG), thereby initiating the photorespiratory (C_2) cycle (Bowes et al., 1971; Ogren and Bowes, 1971). The photorespiratory cycle regenerates 3PGA from 2PG in a complex series of reactions involving at least 16 enzymes and occurring in the cytosol (Timm et al., 2008) and in three organelles (chloroplasts, peroxisomes, and mitochondria), which necessitates the involvement of 14 to 18 transport steps (Leegood et al., 1995; Douce and Neuburger, 1999; Reumann and Weber, 2006). In the mitochondria, the glycine decarboxylase complex (GDC) and serine hydroxymethyltransferase (SHMT) catalyze the photorespiratory conversion of the Gly, derived from 2PG via the activities of phosphoglycolate phosphatase, glycolate oxidase, and an aminotransferase, into Ser, with the concomitant evolution of CO_2 and ammonia (Douce et al., 2001; Bauwe and Kolukisaoglu, 2003). Thus, photorespiration lowers photosynthetic efficiency in that the CO_2 and ammonia must be reassimilated in the chloroplast by Rubisco and the glutamine synthetase (GS)/Ferredoxin-dependent glutamate synthase (Fd-GOGAT) system, respectively, with the concomitant consumption of both ATP and reducing power (Leegood et al., 1995; Douce and Neuburger, 1999; Zhu et al., 2008). This energetic inefficiency means that photorespiration protects against photoinhibition, especially under stress conditions in which CO_2 assimilation is lessened. The generation of CO_2 by photorespiration continues to drive the C_3 cycle, and the combined C_2 and C_3 cycles consume ATP and reducing equivalents, limiting the diversion of light energy into the production of active oxygen species that cause photoinhibition (Kozaki and Takeba, 1996; Wingler et al., 2000).

Forward genetic analysis has been important in the elucidation of the photorespiratory pathway (Somerville, 1986, 2001). Recent supplementation with reverse genetics has allowed the characterization of the last known enzyme of the photorespiratory cycle (Boldt et al., 2005). Although it is likely that some transporters remain incompletely characterized (Weber, 2004; Linka and Weber, 2005), it is tempting to conclude that the photorespiratory cycle is fully characterized. However, the assembly of a parts list does not necessarily constitute a detailed understanding and, by definition, excludes components whose function has not yet been identified.

[1] Current address: Max Planck Institute for Developmental Biology, Department of Molecular Biology, Spemannstrasse 37-39, D-72076 Tübingen, Germany.
[2] Current address: Department of Pharmacology and Cancer Biology, Duke University Medical Center, Box 3813, Durham, NC 27710.
[3] Address correspondence to mcclung@dartmouth.edu.
The author responsible for distribution of materials integral to the findings presented in this article in accordance with the policy described in the Instructions for Authors (www.plantcell.org) is: C. Robertson McClung (mcclung@dartmouth.edu).
[W] Online version contains Web-only data.
www.plantcell.org/cgi/doi/10.1105/tpc.108.063289

Nitrogen metabolism is crucial in photorespiration and the flux through this pathway is ~10-fold greater than the amount of nitrogen assimilated from the soil (Keys et al., 1978). For many years it has been accepted that the reassimilation of photorespiratory ammonia is catalyzed by GS/Fd-GOGAT in the chloroplasts (Leegood et al., 1995; Douce and Neuburger, 1999). The *Arabidopsis thaliana* genome includes two genes encoding distinct Fd-GOGAT isozymes; the photorespiratory function is associated exclusively with *FERREDOXIN-DEPENDENT GLUTAMATE SYNTHASE1* (*GLU1*) (Somerville and Ogren, 1980; Coschigano et al., 1998). Similarly, the completion of the *Arabidopsis* genome sequence indicates that SHMT in *Arabidopsis* is encoded by seven *SHM* genes, two of which encode mitochondrial isoforms (McClung et al., 2000; Bauwe and Kolukisaoglu, 2003). However, only *SHM1* is necessary and sufficient to specify photorespiratory SHMT activity (Voll et al., 2006).

In this work, we uncover an additional level of complexity that further modifies our understanding of photorespiration. We show an unanticipated physical interaction between two of the first photorespiratory pathway components to be identified, SHMT (Somerville and Ogren, 1981) and Fd-GOGAT (Somerville and Ogren, 1980). This interaction was unexpected because photorespiratory SHMT activity is mitochondrial, whereas photorespiratory Fd-GOGAT activity is chloroplastic (Leegood et al., 1995; Douce and Neuburger, 1999). Such spatial separation would seem to preclude a physical interaction. Nonetheless, we provide genetic evidence that *GLU1* is required for mitochondrial SHMT activity through the characterization of a novel *GLU1* allele, *glu1-201*, that retains wild-type Fd-GOGAT activity but is deficient in photorespiratory SHMT activity. Microscopy imaging of green fluorescent protein (GFP) fusions and immunological analysis of biochemically purified organelles show that *GLU1*-encoded Fd-GOGAT is dual targeted to both chloroplasts and mitochondria. We further show that Fd-GOGAT and SHMT1 physically interact in vivo through coimmunoprecipitation and bimolecular fluorescence complementation (BiFC). Thus, we conclude that *GLU1*-encoded Fd-GOGAT associated with the mitochondria is necessary for photorespiratory SHMT activity.

RESULTS

Characterization of a Novel Photorespiratory Mutant Defective in Mitochondrial SHMT Activity

Homozygous *shm1-1* (originally called *stm*; Somerville and Ogren, 1981) mutants exhibit a severe photorespiratory phenotype of lethal chlorosis under low CO_2, and the requirement for supplementary CO_2 is absolute (Voll et al., 2006) (compare Figure 1A, the *glabra1* [*gl1*] mutant that serves as the isogenic wild type to *shm1-1* in Figure 1B; see Supplemental Figures 1A and 1B for seedlings grown at elevated CO_2). By contrast, a second *stm* allele, herein called *glu1-201*, that confers a similar reduction in SHMT activity (Table 1) will grow without added CO_2 in dim (~50 to 75 $\mu mol \cdot m^{-2} \cdot s^{-1}$) light, although the plants are chlorotic and considerably smaller than the wild type (Figure 1C; see Supplemental Figure 1C online). Although we initially attributed this less severe phenotype to a partial loss of *SHM1* function, we failed to identify any nucleotide lesion in the coding sequence and promoter region of *SHM1* in the mutant. Unexpectedly, the F1 progeny from crosses of this second allele with *shm1-1* were not chlorotic in low CO_2 (Figure 1F; see Supplemental Figure 1F online) and showed wild-type levels of SHMT activity (Table 1). This genetic complementation suggests that this mutation, although previously thought to be allelic with *shm1-1*, is a mutation in a distinct gene.

We established that this second mutation maps to a position near the top of chromosome V between the markers CTR1.2 and NGA151, which is distinct from the positions of any of the seven *SHM* genes (Figure 2A). Further analysis using 300 F2 chlorotic plants positioned the mutation close to *GLU1*, which encodes photorespiratory Fd-GOGAT (Coschigano et al., 1998). We therefore tested the hypothesis that our mutation was a novel allele of *GLU1* by genetic complementation. Indeed, introduction into the mutant background of the wild-type *GLU1* gene driven by either the *35S* promoter or the endogenous *GLU1* promoter both rescued the photorespiratory phenotype of chlorosis at low CO_2 (Figures 1G and 1I; see Supplemental Figures 1G and 1I online) and restored wild-type levels of SHMT activity (Table 1). Accordingly, we conclude that this SHMT-defective photorespiratory phenotype is conferred by a novel allele of *GLU1* designated *glu1-201*. Earlier authors called *glu1* mutants *gluS* (Somerville and Ogren, 1980), *gltS* (Suzuki and Rothstein, 1997), or *gls* (Coschigano et al., 1998), but we propose to revise the mutant designation to be consistent with the accepted gene name.

Consistent with the identification of *GLU1* as the gene responsible for the photorespiratory phenotype and loss of SHMT activity in *glu1-201*, there is a single nucleotide change (C6410T) between the wild type and mutant that changes amino acid 1270 from Leu to Phe. Protein gel blot analysis indicates that Fd-GOGAT accumulates to approximately normal levels in *glu1-201* seedlings, consistent with a point mutation that does not disrupt protein accumulation (Figure 3A). SHMT1 protein levels are unaffected in the *glu1-201* mutant, although SHMT1 protein is below detectable levels in the *shm1-1* mutant (Figure 3A). As indicated above, introduction of the wild-type *GLU1* gene driven by either its endogenous promoter or the 35S promoter into *glu1-201* rescues the photorespiratory chlorosis phenotype and restores wild-type levels of SHMT activity (Figures 1G and 1I, Table 1; see Supplemental Figures 1G and 1I online). However, introduction of a modified *GLU1* carrying the L1270F mutation driven by the *35S* promoter into *glu1-201* fails to rescue chlorosis or to restore wild-type levels of SHMT activity (Figure 1L, Table 1; see Supplemental Figure 1L online) in plants growing at ambient CO_2 levels, consistent with this mutation conferring the photorespiratory phenotype.

Loss-of-function mutations in *GLU1* had been previously demonstrated to exhibit photorespiratory chlorosis and loss of Fd-GOGAT activity (Somerville and Ogren, 1980; Suzuki and Rothstein, 1997; Coschigano et al., 1998). We confirmed that a T-DNA insertion mutant (Salk_104286, termed *glu1-202*), in which the T-DNA has inserted into the 2nd exon of *GLU1*, lacks Fd-GOGAT protein (Figure 3A) and exhibits reduced Fd-GOGAT activity (Table 1) and photorespiratory chlorosis (compare Figure

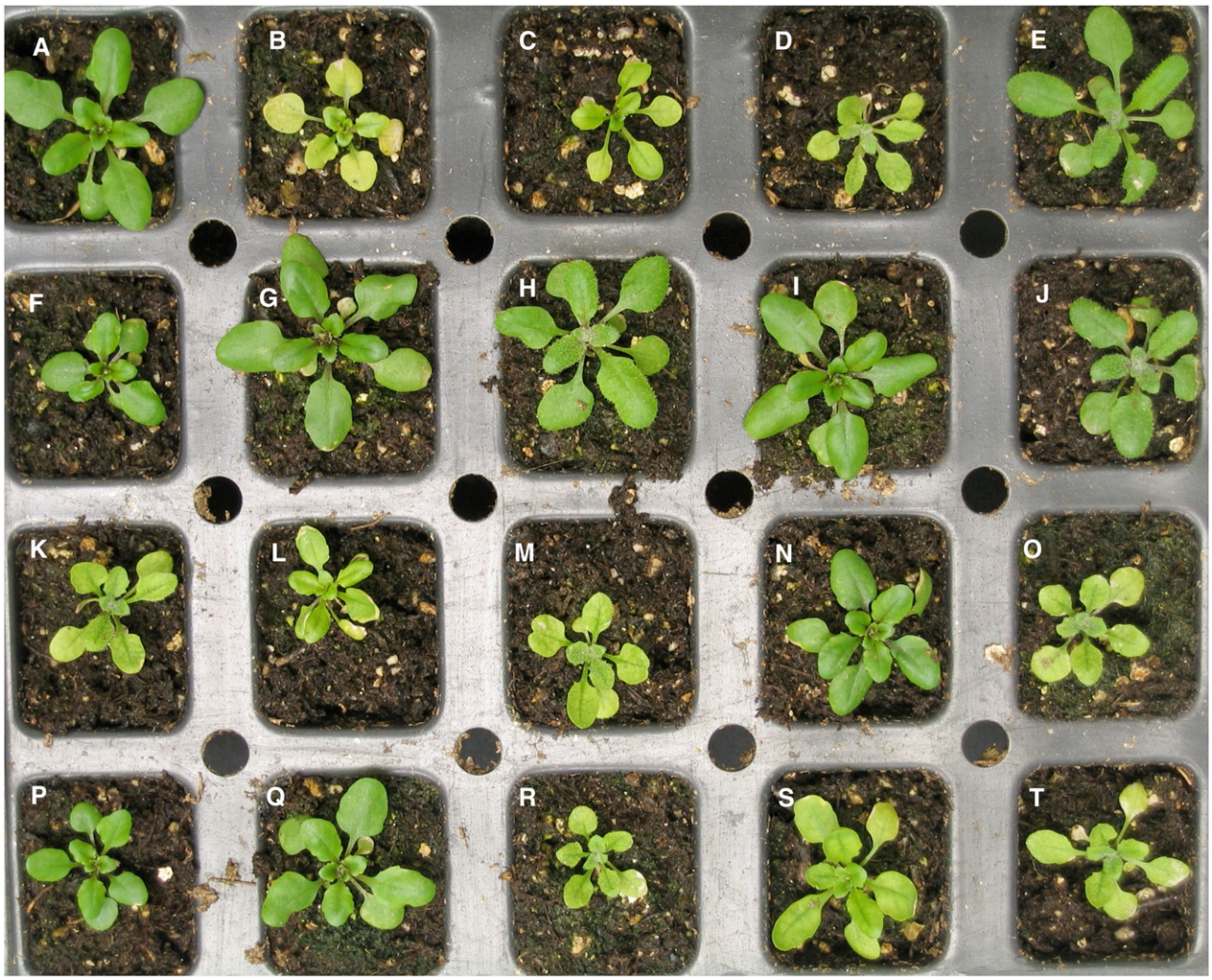

Figure 1. Phenotypic Analysis of Photorespiratory Mutants at Ambient CO_2.

Seedlings were grown at elevated (3%) CO_2 levels for 10 d at 22°C in long days (16 h light at 100 μmol·m^{-2}·s^{-1}: 8 h dark) and then transferred to ambient CO_2 for 5 d.

(A) *glabra1* (Col), the isogenic parent to *shm1-1* and *glu1-201*; **(B)** *shm1-1*; **(C)** *glu1-201*; **(D)** *glu1-202*; **(E)** Col-0, the isogenic parent to *glu1-202*; **(F)** F1: *shm1-1* × *glu1-201*; **(G)** *glu1-201/p35S:GLU1*; **(H)** *glu1-202/P35S:GLU1*; **(I)** *glu1-201/PGLU1:GLU1*; **(J)** *glu1-202/PGLU1:GLU1*; **(K)** F1: *glu1-201* × *glu1-202*; **(L)** *glu1-201/P35S:glu1*^{L1270F}; **(M)** *glu1-202/P35S:glu1*^{L1270F}; **(N)** *glu1-201/P35S:glu1*^{204}; **(O)** *glu1-202/P35S:glu1*^{204}; **(P)** *glu1-201* / *Pmas:GLU1*; **(Q)** *glu1-201/Pmas:glu1*^{M1K}; **(R)** *glu1-202/Pmas:glu1*^{M1K}; **(S)** *glu1-201/Pmas:glu1*^{M3I}; **(T)** *glu1-202/Pmas:glu1*^{M3I}.

1D with the isogenic wild type, Columbia-0 [Col-0], in Figure 1E and Supplemental Figures 1D and 1E online). This allele also confers a reduction in SHMT activity (Table 1). The *glu1-202* mutant is fully rescued by expression of wild-type *GLU1* but not by *glu1*^{L1270F} under control of the *35S* promoter (Figures 1H, 1J, and 1M, Table 1; see Supplemental Figures 1H, 1J, and 1M online). The F1 plants resulting from a cross between *glu1-201* and *glu1-202* display photorespiratory chlorosis and reduced SHMT activity, indicating that the two mutations are allelic (Figure 1K, Table 1; see Supplemental Figure 1K online).

glu1-201 has reduced SHMT activity but retains wild-type levels of Fd-GOGAT activity, suggesting that the positive effect of *GLU1* on SHMT activity is independent of Fd-GOGAT catalytic activity. To test this, we generated a new allele of *GLU1*, *glu1*^{204}, in which residues 299 to 1007, including the central domain and parts of the N-terminal aminotransferase domain and the FMN binding domain, are deleted in frame (Figure 2C). The *glu1*^{204} allele fails to rescue either photorespiratory chlorosis or Fd-GOGAT activity when introduced into *glu1-202* (Figure 1O, Table 1; see Supplemental Figure 1O online), consistent with its predicted lack of Fd-GOGAT catalytic activity. However, the *glu1*^{204} allele fully rescues photorespiratory chlorosis and SHMT activity when introduced into the *glu1-201* mutant (Figure 1N, Table 1; see Supplemental Figure 1N online). Thus, we conclude that wild-type levels of photorespiratory SHMT activity require Fd-GOGAT expression (although not catalytic activity) and that a

Table 1. Phenotypic analysis of photorespiratory mutants.

Genotype/Transgene	SHMT Activity nmol mg^{-1} min^{-1}	Fd-GOGAT Activity nmol mg^{-1} min^{-1}	Chlorosis in Low CO_2
Col-0	1.64 ± 0.07	45 ± 1.1	No
shm1-1	0.18 ± 0.01	40 ± 1.5	Yes
shm1-1/P35S:SHM1	1.60 ± 0.06	44 ± 2.7	No
shm1-1/PSHM1:SHM1	1.65 ± 0.10	46 ± 2.1	No
glu1-201	0.20 ± 0.02	43 ± 2.2	Yes
glu1-201/P35S:GLU1	1.51 ± 0.09	46 ± 1.5	No
glu1-201/PGLU1:GLU1	1.62 ± 0.08	48 ± 1.7	No
glu1-201/P35S:glu1^{L1270F}	0.25 ± 0.09	44 ± 1.8	Yes
glu1-201/P35S:glu1^{204}	1.60 ± 0.08	47 ± 3.2	No
glu1-201/Pmas:GLU1	1.57 ± 0.07	46 ± 1.2	No
glu1-201/Pmas:glu1^{M1K}	1.82 ± 0.04	44 ± 1.9	No
glu1-201/Pmas:glu1^{M3I}	0.27 ± 0.07	16 ± 0.5	Yes
glu1-202	0.62 ± 0.05	15 ± 0.5	Yes
glu1-202/P35S:GLU1	1.49 ± 0.08	45 ± 1.1	No
glu1-202/P35S:glu1^{L1270F}	0.29 ± 0.06	49 ± 1.6	Yes
glu1-202/Pmas:glu1^{M1K}	1.71 ± 0.10	17 ± 0.9	Yes
glu1-202/Pmas:glu1^{M3I}	0.30 ± 0.06	46 ± 1.3	Yes
glu1-202/P35S:glu1^{204}	1.55 ± 0.09	15 ± 0.03	Yes
F1: *shm1-1* × *glu1-201*	1.50 ± 0.01	46 ± 1.7	No
F1: *glu1-202* × *glu1-201*	0.43 ± 0.06	45 ± 2.1	Yes

Phenotypic analysis of photorespiratory mutants grown at elevated (3%) CO_2 levels for 10 d at 22°C in long days (16 h white light at 100 $\mu mol \cdot m^{-2} \cdot s^{-1}$: 8 h dark) and then transferred to ambient CO_2 levels for 5 d. Enzymes are presented as mean ± SD based on at least two biological replicates, each with at least three technical replicates. *Pmas* indicates the *A. tumefaciens mas* promoter. All genotypes presented in this table were confirmed by sequencing of regions diagnostic for either the endogenous or the transgenic locus (see Supplemental Figure 2 online).

mutation of L1270F results in a *glu1* species that is unable to sustain wild-type SHMT activity, even though it retains wild-type Fd-GOGAT activity.

Dual Targeting of Fd-GOGAT to the Mitochondria in Addition to the Chloroplasts

It is surprising and puzzling that the wild-type *GLU1* gene, which encodes a chloroplastic Fd-GOGAT (Suzuki and Rothstein, 1997; Coschigano et al., 1998; Lee et al., 2008), rescues a mutant lacking mitochondrial SHMT activity (Somerville and Ogren, 1981). Because Fd-GOGAT catalytic activity is not required for this rescue, we speculated that perhaps a physical interaction between SHMT and Fd-GOGAT might be necessary for full SHMT activity. Such a physical interaction would require common localization of Fd-GOGAT and SHMT1, which seemed unlikely as photorespiratory SHMT activity is known to be mitochondrial (Somerville and Ogren, 1981), whereas photorespiratory Fd-GOGAT activity is chloroplastic (Somerville and Ogren, 1980). At this time, the Subcellular Proteomics Database does not provide proteomic data to support a mitochondrial localization of Fd-GOGAT (Heazlewood et al., 2007). Therefore, to verify these localizations, we performed microscopy analyses and biochemical fractionation experiments.

First, we made C-terminal GFP fusions to SHMT1 and to Fd-GOGAT in constructs driven by the endogenous *SHM1* and *GLU1* promoters, respectively. These transgenes were introduced into *shm1-1* and *glu1-201* seedlings to yield stably transformed lines. Each GFP fusion construct rescued the photorespiratory defect of the corresponding loss-of-function mutant. Protoplasts were generated from leaves of these rescued lines and analyzed by fluorescence microscopy. SHMT1-GFP showed green punctate fluorescence (Figure 4A) that colocalized with fluorescence from the MitoTracker Red mitochondrial marker (Figures 4B and 4C), confirming that SHMT1 is targeted to the mitochondria. As expected, Fd-GOGAT-GFP showed chloroplastic localization (cf. the GFP fluorescence Figure 4E with the differential interference contrast image of Figure 4H). Unexpectedly, Fd-GOGAT-GFP also showed green punctate fluorescence (Figure 4E) that colocalized with the MitoTracker Red mitochondrial marker (Figures 4F and 4G). This result indicates that Fd-GOGAT is targeted to both the chloroplasts and the mitochondria.

Second, we performed biochemical fractionation experiments to confirm our microscopy observations. Fd-GOGAT was detected by protein gel blot analysis of wild-type Col seedlings in both chloroplastic and mitochondrial fractions (Figure 3B). By contrast, SHMT1 was detected in mitochondrial but not in chloroplastic fractions. As expected, the photosystem II chlorophyll binding protein D1 PSBA was detected in chloroplastic but not in mitochondrial fractions (Figure 3B). These data are consistent with our microscopy localizations of GFP fusion proteins. Therefore, we conclude that Fd-GOGAT is dual targeted to both chloroplasts and mitochondria.

An increasing number of examples have been described in which proteins are dual targeted to both the chloroplast and mitochondrion (Small and Peeters, 2001; Mackenzie, 2005). Dual targeting is typically accomplished by the presence of tandem

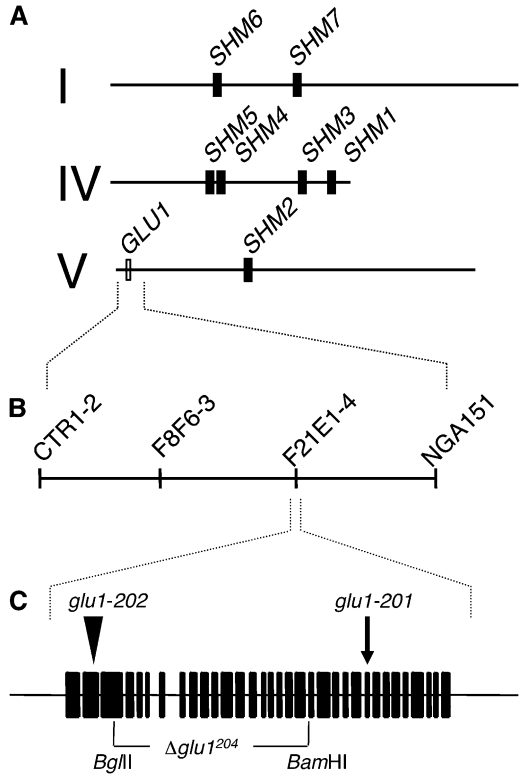

Figure 2. Positional Cloning of *glu1-201* (Originally *stm*, CS8010).

(A) Map position of *SHM* genes (on chromosomes I, IV, and V) and *GLU1* (on chromosome V).
(B) Partial genetic map of chromosome V between CTR1-2 and NGA151.
(C) Structure of the Fd-GOGAT (*GLU1*) gene, as well as the position of the point mutation in *glu1-201* (L1270F), of a T-DNA insertion into the second exon in *glu1-202* (Salk_104286), and of the in-frame deletion between the *Bgl*II and *Bam*HI sites in *glu1*^{204}. Exons are represented by boxes, and introns are indicated by lines.

chloroplastic and mitochondrial targeting sequences or else by the presence of an ambiguous presequence that is recognized by the import apparatus of both organelles. We hypothesized that Fd-GOGAT may be dual targeted to mitochondria and chloroplasts by use of multiple translation starts (Richter et al., 2002). Inspection of the sequence of Fd-GOGAT revealed two Met residues representing potential translation initiation sites at positions 1 and 3. Computer predictions (PSORT and TargetP; Emanuelsson et al., 2000; Bannai et al., 2002) suggested that initiation at the first ATG codon would allow chloroplastic targeting, whereas initiation at the second ATG would confer mitochondrial targeting. Accordingly, we generated three constructs based on the *GLU1* cDNA fused in frame to GFP and driven by the *GLU1* promoter. The first encodes simply the wild-type Fd-GOGAT sequence (MAM) and is predicted to be targeted to the chloroplast (see Supplemental Figure 3 online). The second construct, Fd-GOGAT^{M1K} (KAM), would be translated from the second Met and is predicted to be targeted to the mitochondrion. The third, Fd-GOGAT^{M3I} (MAI), is predicted to be targeted to the chloroplast. All three clones were transformed into the *glu1-201* mutant. We first tested for subcellular localization in protoplasts derived from stable transformants carrying the three constructs. As predicted, Fd-GOGAT and Fd-GOGAT^{M1K} show punctate fluorescence that colocalizes with the mitochondrial marker (Figures 4E to 4L), whereas Fd-GOGAT^{M3I} shows chloroplastic and not mitochondrial localization (Figures 4M to 4P). The transgenic *glu1-201* plants carrying *Pmas:glu1*^{M1K} and *PGLU1:GLU1* are rescued to a wild-type phenotype under photorespiratory (ambient CO_2) conditions and express wild-type levels of SHMT activity (Figures 1I and 1Q, Table 1; see Supplemental Figures 1I and 1Q online). Similarly, *glu1*^{M1K} lacking the C-terminal GFP and driven from the *Agrobacterium tumefaciens mannopine synthase* (*mas*) promoter rescued *glu1-201* plants to a wild-type phenotype under photorespiratory (ambient CO_2) conditions (Figure 1Q, Table 1; see Supplemental Figure 1Q online). However, those *glu1-201* plants transformed with *Pmas:glu1*^{M3I} remain chlorotic at ambient CO_2 and have low SHMT activity (Figure 1S, Table 1; see Supplemental Figure 1S online). This is consistent with a requirement for Fd-GOGAT to be targeted to the mitochondria to play its role in expression of wild-type levels of SHMT activity. The photorespiratory chlorosis of *glu1-202* plants was not rescued by *Pmas:glu1*^{M1K} (Figure 1R, Table 1; see Supplemental Figure 1R online) but was rescued by *Pmas:glu1*^{M3I} (Figure 1T, Table 1; see Supplemental Figure 1T online).

Dual targeting has also been shown to result from upstream translation from non-ATG start codons to generate a mitochondrial isoform, while translation from the ATG yields a chloroplastic isoform (Christensen et al., 2005). Interestingly, *GLU1* has an in-frame GTG alternate initiation codon at position −17. We tested the importance of upstream translation to Fd-GOGAT dual targeting with two further constructs (see Supplemental Figure 3 online). In one, *Pmas:glu1*^{M1KM31}, we mutagenized both ATG start codons. This construct would be expected to rescue either *glu1-201* or *glu1-202* seedlings if translation from the upstream GTG codon could yield a mitochondrial or a chloroplastic Fd-GOGAT isoform, respectively. However, *Pmas:glu1*^{M1KM31} does not rescue either mutant (see Supplemental Figure 3 online). In

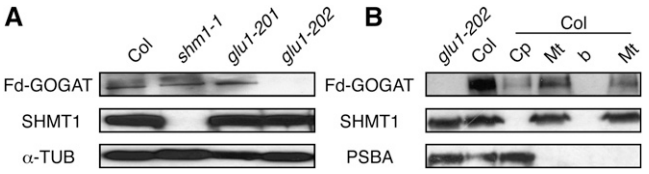

Figure 3. Accumulation of Fd-GOGAT and SHMT1 Protein in Whole Seedlings and in Subcellular Fractions of Leaves.

(A) Accumulation of Fd-GOGAT and SHMT1 protein in whole extracts (20 μg of whole leaf extract per sample) prepared from wild-type and mutant seedlings. α-Tubulin (α-TUB) serves as a loading control.
(B) Accumulation of Fd-GOGAT and SHMT1 protein in chloroplast (Cp) and mitochondrial (Mt) fractions (20 μg per sample) of wild-type Col seedlings. Whole seedling extracts from Col and *glu1-202* are shown as controls. b indicates a blank lane containing no extract. The photosystem II chlorophyll binding protein D1 (PSBA) serves as a loading control. For both **(A)** and **(B)**, similar results were obtained from two experiments using separate extracts from independently grown plants.

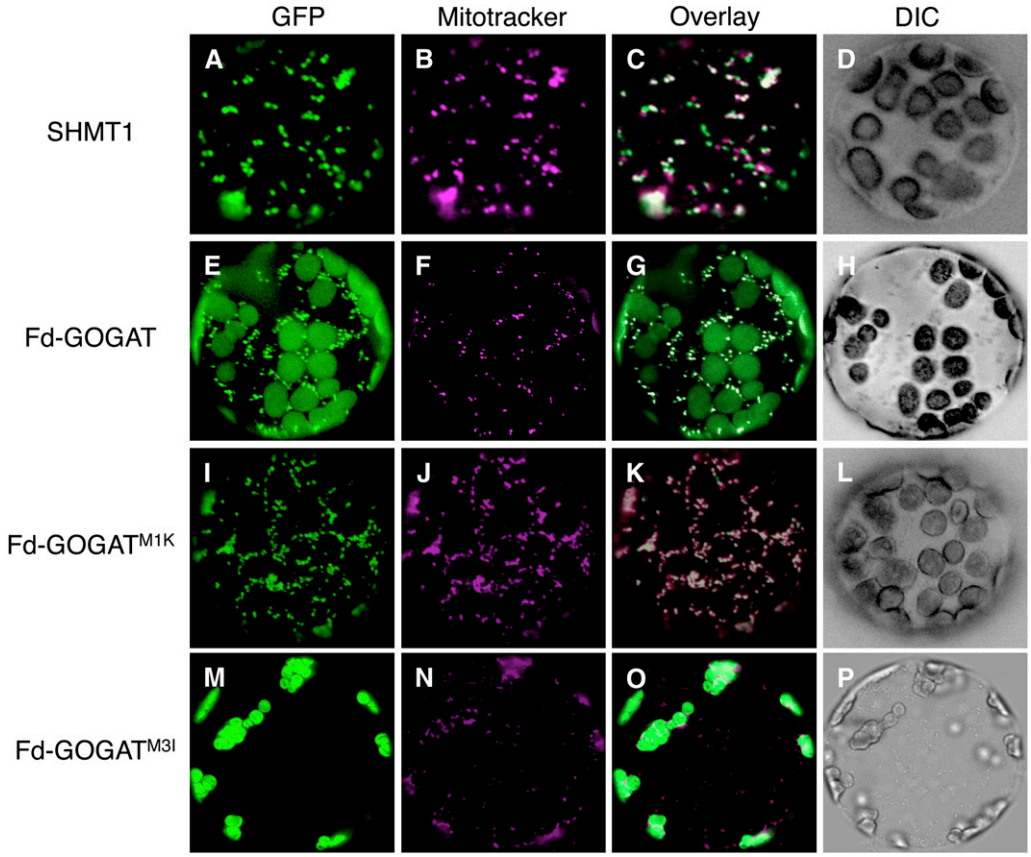

Figure 4. Microscopy Analysis of Subcellular Localization of Fd-GOGAT and SHMT1.

Protoplasts prepared from *shm1-1* (**[A]** to **[D]**) or *glu1-201* (**[E]** to **[P]**) plants stably transformed to carry *PSHM1:SHM1:GFP* (**[A]** to **[D]**), *PGLU1:GLU1:GFP* (**[E]** to **[H]**), *PGLU1:glu1^{M1K}:GFP* (**[I]** to **[L]**), or *PGLU1:glu1^{M3I}:GFP* (**[M]** to **[P]**) were imaged to visualize GFP fluorescence (**[A]**, **[E]**, **[I]**, and **[M]**). Protoplasts were stained with Mitotracker to show the mitochondria (**[B]**, **[F]**, **[J]**, and **[N]**). The overlay of GFP and Mitotracker signals is shown in **(C)**, **(G)**, **(K)**, and **(O)**. Differential interference contrast (DIC) images are shown in **(D)**, **(H)**, **(L)**, and **(P)**. Protoplasts (100 to 200) of each genotype were examined on at least five occasions, and representative images are presented.

the second construct, we introduced a stop codon at position −6, in between the upstream GTG start and the ATG start codons at positions 1 and 3. If translation from the upstream GTG were required for dual targeting, then this construct, *Pmas:glu1^{-6STOP}*, would not be expected to rescue both *glu1-201* and *glu1-202*. However, *Pmas:glu1^{-6STOP}* rescues both mutants (see Supplemental Figure 3 online). Therefore, we conclude both that upstream translation initiation is not necessary for dual targeting of Fd-GOGAT to both chloroplasts and mitochondria and that upstream translation initiation is not sufficient to yield enough Fd-GOGAT to support either its mitochondrial or its chloroplastic photorespiratory functions.

SHMT and Fd-GOGAT Interact in Vivo

One hypothesis to explain the requirement of mitochondrial Fd-GOGAT for photorespiratory SHMT activity is that Fd-GOGAT forms physical complexes with SHMT. To test this hypothesis, we performed coimmunoprecipitation on mitochondria purified from leaf extracts by Percoll density centrifugation using an antibody against SHMT to immunoprecipitate SHMT1 and any interacting proteins. We probed those immunoprecipitates with an antibody against Fd-GOGAT (Figure 5A). To test for the presence of Fd-GOGAT and SHMT, input extracts were probed with antibodies against Fd-GOGAT and SHMT as well as with an antibody against the β-subunit of the inner mitochondrial membrane F1-ATPase as a loading control (Figure 5B). As can be seen in Figure 5A, Fd-GOGAT was coimmunoprecipitated with SHMT1 from wild-type Col extracts, indicating that these two proteins form a complex in wild-type leaves. In the absence of SHMT1 in the *shm1-1* mutant, Fd-GOGAT was not coimmunoprecipitated, indicating that the coimmunoprecipitation is dependent upon SHMT1 protein and not due to cross-reaction with another protein. The specificity of our assay for *GLU1*-encoded Fd-GOGAT is established by the failure to coimmunoprecipitate Fd-GOGAT protein from the *glu1-202* mutant (Figure 5A), which lacks photorespiratory Fd-GOGAT (Figure 3, Table 1). Expression of *GLU1* driven by the 35S promoter in the *glu1-202* background restores Fd-GOGAT protein capable of coimmunoprecipitation with SHMT1 (Figure 5A), consistent with its full

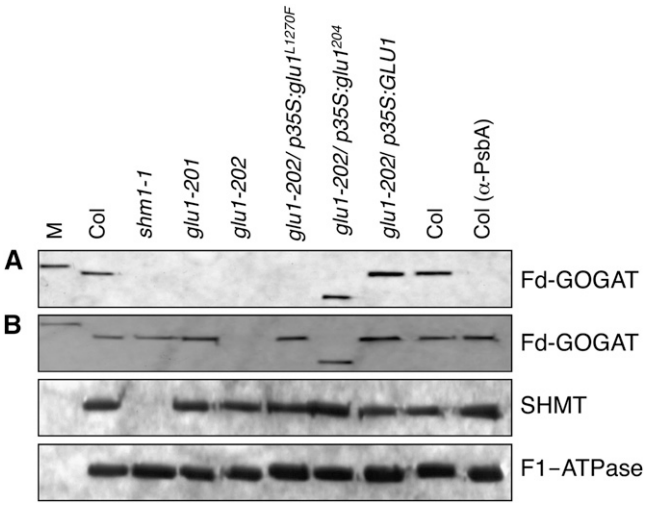

Figure 5. SHMT1 and Fd-GOGAT Interact.

(A) Coimmunoprecipitation assay of Fd-GOGAT with SHMT1. Protein extracts from mitochondria isolated by Percoll density gradient centrifugation from seedlings of the indicated genotypes were incubated with antisera against SHMT1 or the photosystem II chlorophyll binding protein D1 (PsbA) (indicated by Col [α-PsbA], a negative control), and precipitated immunocomplexes were separated by 8% SDS-PAGE. Protein gel blots were stained with an α-Fd-GOGAT antibody. M indicates the marker lane; the anti-Fd-GOGAT antibody strongly cross-reacts with the 200-kD marker protein. Coimmunoprecipitations were performed on two independent extracts for each genotype with similar results.

(B) Input for the coimmunoprecipitations probed with antibodies directed against Fd-GOGAT (top panel), SHMT (middle panel), or β- F1-ATPase (bottom panel).

rescue of the photorespiratory phenotype (Figure 1H, Table 1; see Supplemental Figure 1H online). The L1270F mutation in *glu1-201* eliminates coimmunoprecipitation of Fd-GOGAT with SHMT1 (Figure 5A), consistent with the photorespiratory phenotype (Figure 1C, Table 1; see Supplemental Figure 1C online), despite the presence of wild-type levels of Fd-GOGAT (Figures 3 and 5B). This result implicates this residue (L1270) in a role critical for interaction with SHMT1 and suggests that the photorespiratory phenotype associated with the *glu1-201* mutation results from a loss of interaction of Fd-GOGAT with SHMT1. The *glu1*^{204} deletion of ~2 kb of coding sequence, which eliminates regions required for known catalytic function, does not prevent interaction of Fd-GOGAT with SHMT1, as indicated by the immunoprecipitation of a truncated (~100 kD) Fd-GOGAT species (Figure 5A). This is consistent with the ability of *glu1*^{204} to rescue the photorespiratory phenotype of *glu1-201* (Figure 1N, Table 1; see Supplemental Figure 1N online) and implicates the C-terminal region of Fd-GOGAT, which includes L1270, in that interaction.

To independently test the in vivo interaction of Fd-GOGAT with SHMT, we performed BiFC (Walter et al., 2004). We fused *GLU1* and *SHM1* to the N and C termini, respectively, of *YFP* and transfected the constructs singly or together into Col-0 protoplasts. YFP was placed at the C termini of the constructs to allow the Fd-GOGAT and SHMT1 targeting signals to confer normal subcellular localization. Neither construct alone yielded fluorescence, but when the two constructs were cotransfected, we observed punctate fluorescence that colocalized with the mitochondria (Figure 6). Thus, we conclude that Fd-GOGAT interacts with SHMT1 in vivo.

DISCUSSION

This work has yielded unanticipated results that enrich our understanding of the photorespiratory pathway. We provide genetic, microscopy, and biochemical evidence that the *GLU1*-encoded photorespiratory isoform of Fd-GOGAT is dual targeted to the mitochondria and to the chloroplasts. Genetic evidence indicates that Fd-GOGAT is required for mitochondrial SHMT activity. Coimmunoprecipitation and BiFC experiments establish that Fd-GOGAT complexes with SHMT1 and the physical interaction of Fd-GOGAT with SHMT in the mitochondria is necessary for wild-type levels of SHMT activity.

Although it is widely acknowledged that photorespiration is a complicated pathway with many components, it had been thought that the chief remaining gaps in our knowledge lay in the transporters responsible for interorganellar shuttling of photorespiratory intermediates (Reumann and Weber, 2006). However, our work and other recent studies demonstrate that a detailed mechanistic understanding of the photorespiratory pathway remains to be achieved, and additional complexities may yet emerge. For example, it was recently established that 10-formyl tetrahydrofolate deformylase (10-FDF) is essential for photorespiration (Collakova et al., 2008). In addition, it was recently shown that a novel cytosolic hydroxypyruvate reductase, in addition to the long-known HPR peroxisomal isoform, is important in conversion of hydroxypyruvate to glycerate (Timm et al., 2008), thereby expanding the realm of photorespiratory metabolism into the cytosol in addition to the long-known organellar (chloroplast, peroxisome, and mitochondrion) domains.

In recent years, it has become clear that a number of proteins encoded by nuclear genes are dual targeted, with the chloroplasts/mitochondria being the most common dual destinations (Silva-Filho, 2003; Mackenzie, 2005). Dual plastid/mitochondrion targeting can be achieved either with twin presequences or with an ambiguous presequence. Twin presequences are typically arranged in tandem and distinct isoforms with one or the other presequence generated either via alternative transcriptional starts, alternative splicing, or alternative translation initiation. Ambiguous presequences are capable of interacting with both mitochondrial and plastidic import mechanisms. Our data suggest that Fd-GOGAT employs the twin-presequence mechanism, although the data do not absolutely exclude an ambiguous presequence. Fd-GOGAT initiates with the amino acid triplet MAM. Mutation of the first M to K prevents chloroplast targeting, indicating that translation initiating at the second M yields an isoform restricted to the mitochondria. Mutation of the second M blocks mitochondrial targeting and yields an isoform restricted to the chloroplast. This is consistent with the twin, albeit overlapping, presequence model, but it cannot exclude the ambiguous presequence model in which initiation at the first M yields

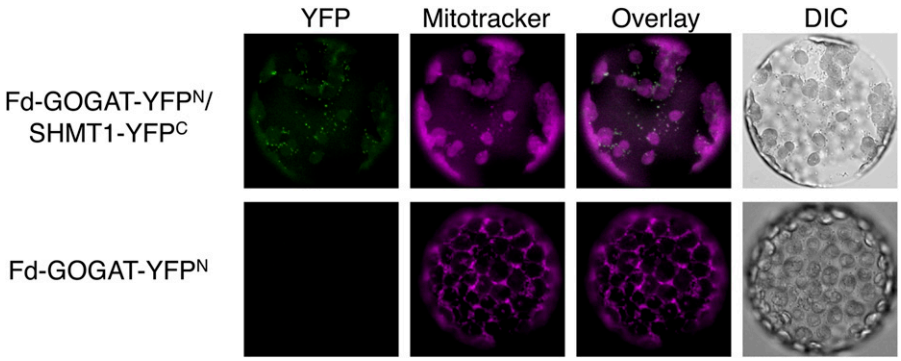

Figure 6. SHMT1 and Fd-GOGAT Interact in Vivo.

BiFC assay. The full-length *GLU1* cDNA was fused to YFP^N, and the full-length *SHM1* was fused to YFP^C. Wild-type mesophyll protoplasts were cotransfected with the Fd-GOGAT-YFP^N and SHMT-YFP^C fusion constructs (top set of panels) or with the Fd-GOGAT-YFP^N fusion construct alone (bottom set of panels). Protoplasts (100 to 200) transformed with the YFP constructs either singly or together were examined for each of two independent transformations, and representative images are presented. DIC, differential interference contrast.

an isoform that interacts with both targeting machineries. In this model, mutation of the second M would disrupt the mitochondrial targeting sequence but leave the chloroplast targeting sequence intact. Translation would not normally occur at the second M, but mutation of the first M would yield a transcript that could be translated from the second M. The distinction between the twin and ambiguous presequence models is that translation from the second M would be integral to the former and only occur as an artifact of our experimental mutation of the first M in the latter. Our data do not allow us to distinguish between these two alternatives.

Why might the mitochondrial fraction of Fd-GOGAT have escaped detection for so long? Fd-GOGAT is well established as a chloroplastic enzyme (Lea and Miflin, 1974), and it is highly abundant, representing ~1% of total leaf protein (Márquez et al., 1988; Pajuelo et al., 1997). Thus, it would have been easy to attribute any Fd-GOGAT identified in other compartments, including the mitochondria, to contamination from the chloroplast fraction. In this regard, it is interesting to note that while pea (*Pisum sativum*) leaf mitochondrial SHMT purifies as a 220-kD homotetramer (Bourguignon et al., 1988; Turner et al., 1992), in less pure fractions, SHMT activity can be resolved into two distinct fractions (Turner et al., 1992). Thus, it is possible that a complex of SHMT and Fd-GOGAT might have been seen in earlier preparations but that the Fd-GOGAT/SHMT1 complex was lost in purification.

Intriguingly, *GLN2*-encoded GS-2 was recently suggested to be dual targeted to the mitochondria in addition to the chloroplasts (Taira et al., 2005). This raises the possibility that ammonia, which is generated by GDC activity in the mitochondria (Douce et al., 2001; Bauwe and Kolukisaoglu, 2003), may be reassimilated in the mitochondria (Linka and Weber, 2005; Taira et al., 2005). However, GS is depleted from mitochondrial fractions highly purified by free-flow electrophoresis (FFE) relative to pre-FFE mitochondrial fractions, suggesting that it was primarily detected as a plastidic contaminant of incompletely purified mitochondrial fractions (Eubel et al., 2007). FFE provides a second dimension of organellar resolution based on surface charge, thus augmenting conventional separations based on centrifugation to resolve by size and density. Although we detected Fd-GOGAT in mitochondria purified by Percoll density gradient centrifugation (Figure 3B), FFE-purified Col-0 shoot mitochondria and Landsberg *erecta* tissue culture mitochondria do not contain sufficient amounts of Fd-GOGAT to be detected by mass spectrometry or by protein gel blots using Fd-GOGAT antibodies (H. Millar and C.P. Lee, personal communication). One interpretation of this failure to find Fd-GOGAT by proteomic techniques is that Fd-GOGAT in the mitochondrial fraction results from plastidic contamination. However, this interpretation is inconsistent with our evidence supporting a mitochondrial fraction of Fd-GOGAT based on multiple independent experimental approaches (genetic, biochemical, and microscopy evidence). We offer two possible explanations to reconcile these different observations. One possibility is that mitochondrial Fd-GOGAT is scarce, which would be consistent with a catalytic rather than a stoichiometric role of Fd-GOGAT in mitochondria. A second possibility is that Fd-GOGAT is present in a subset of a heterogeneous mitochondrial population and that this Fd-GOGAT-containing subset is lost during FFE purification. For example, distinct yeast mitochondrial populations originating from different biological conditions or experimental manipulations can be resolved by FFE and as little as deletion of a single outer-membrane protein can yield a mitochondrial fraction of distinct mobility in FFE (Zischka et al., 2006).

The ability of $glu1^{204}$, an internally deleted Fd-GOGAT isoform lacking the catalytic region of the protein, to rescue the photorespiratory SHMT activity of a *glu-201* mutant (Figure 1N, Table 1; see Supplemental Figure 1N online) demonstrates that the mitochondrial role does not require Fd-GOGAT catalytic activity. Fd-GOGAT is a large four-domain protein, although no function has been attributed to the C-terminal domain (Binda et al., 2000; van den Heuvel et al., 2002). The *glu1-201* mutation (L1270F) confers the loss of photorespiratory SHMT activity (Figure 1C, Table 1; see Supplemental Figure 1C online), presumably by preventing the interaction of Fd-GOGAT with SHMT1. This result assigns an important photorespiratory function, the mediation

of the interaction between Fd-GOGAT and SHMT1, to the C-terminal domain of Fd-GOGAT.

The mechanistic function of the SHMT-Fd-GOGAT interaction remains speculative. The binding of Fd-GOGAT is not necessary to stabilize SHMT1 protein because SHMT1 protein levels are not reduced in the *glu1-201* or *glu1-202* mutants (Table 1). In vitro SHMT activity is not dependent on Fd-GOGAT, so this requirement seems to be restricted to the in vivo situation. One model for a noncatalytic role of Fd-GOGAT in a complex with SHMT is as an in vivo regulatory subunit whose function is independent of Fd-GOGAT activity. *O*-acetylserine(thiol)-lyase has been shown to play such a regulatory role in the Cys synthase complex with serine acetyltransferase (SAT). Although it was proposed that this complex promotes metabolic channeling (Winkel, 2004), it was demonstrated using recombinantly produced enzymes that *O*-acetylserine(thiol)-lyase binds to SAT as a catalytically inactive enhancer of SAT activity (Ruffet et al., 1994; Droux et al., 1998). There is precedent for Fd-GOGAT playing a role independent of catalytic activity. Fd-GOGAT participates in a large multimeric complex with UDP-sulfoquinovose synthase (SQD1) (Shimojima et al., 2005). This role apparently does not require glutamate synthase catalytic activity of Fd-GOGAT but is thought to rely on an FMN cofactor that binds sulfite and may channel it to SGD1. Nonetheless, we do not favor this model because the low abundance of Fd-GOGAT in the mitochondrion suggests that only a small fraction of the SHMT is likely to be complexed with Fd-GOGAT.

We propose a catalytic role for Fd-GOGAT in the mitochondria, which would be consistent with an essential function for an inabundant protein. What catalytic role, independent of GOGAT activity, might Fd-GOGAT bound to SHMT1 play? It has been known for some years that SHMT plays a second catalytic role, the irreversible hydrolysis of 5,10-methenyl tetrahydrofolate (5,10-CH=THF) to 5-formyl tetrahydrofolate (5-CHO-THF), which is a slow tight binding inhibitor of SHMT (Stover and Schirch, 1993). It has been recently established that two 10-FDF oppose the accumulation of 5-CHO-THF, and a double loss-of-function mutant confers a photorespiratory phenotype via inhibition of SHMT and GDC activities, confirming the importance of this inhibitor in vivo (Collakova et al., 2008). 5-CHO-THF is metabolized back to 5,10-CH=THF by 5-formyltetrahydrofolate cycloligase, encoded in *Arabidopsis* by a single *5-FCL* gene (Roje et al., 2002). However, the loss of 5-FCL activity does not dramatically reduce plant growth under photorespiratory conditions, despite the accumulation of 5-CHO-THF (Goyer et al., 2005). No compensatory increase in mitochondrial SHMT activity could be detected in the 5-FCL mutants, suggesting some other mechanism to tolerate elevated 5-CHO-THF (Goyer et al., 2005). We speculate that the role of Fd-GOGAT bound to SHMT1 may be to reduce the sensitivity of SHMT activity to 5-CHO-THF or to oppose the accumulation of 5-CHO-THF, possibly by reducing the hydrolysis of of 5,10-CH=THF by SHMT. This would be consistent with the loss of SHMT activity in *glu1-201* despite the retention of wild-type levels of SHMT protein.

While all primary enzymes and several of the transporters required for a functional C_2 carbon oxidative cycle have now been identified, the resulting parts list apparently does not yet permit one to draw a complete picture of this crucial high flux pathway in photosynthetic plant cells. As we and others have shown, a functional pathway requires more than the sum of its parts and, in addition, more parts than previously anticipated (e.g., Collakova et al., 2008). Protein–protein interactions and complex formation are required for mitochondrial SHMT activity, and this requires mitochondrial targeting of an enzyme, Fd-GOGAT, that was hitherto believed to be confined to chloroplasts. We conclude that this crucial high flux pathway is more complicated than anticipated and remains incompletely understood.

METHODS

Plant Growth

Seeds of the *glu1-201* mutant (CS8010) and of the Salk T-DNA-Insertion line Salk_104286, *glu1-202*, were obtained from the ABRC (Ohio State University, Columbus, OH). Seeds were grown on soil in high (3%) CO_2 growth chambers (Biochambers) at 22°C in long days (16 h white light at 100 $\mu mol \cdot m^{-2} \cdot s^{-1}$: 8 h dark). For mapping, seeds were vapor sterilized (Clough and Bent, 1998) and germinated at room temperature in a 12-h-light/12-h-dark cycle on half-strength Murashige and Skoog medium (Murashige and Skoog, 1962) in 3% CO_2 in white light at a photon flux density of $\sim$100 $\mu mol \cdot m^{-2} \cdot s^{-1}$. Plantlets were transferred to soil after the first four primary leaves had emerged and grown at 22°C in long days (16 h white light at 100 $\mu mol \cdot m^{-2} \cdot s^{-1}$: 8 h dark) at ambient CO_2 to score photorespiratory chlorosis. The plants were returned to the 3% CO_2 growth chamber and the growth cycle was completed.

Mapping of the *glu1-201* Locus

The homozygous recessive mutant *glu1-201* (Col *gl1*) was crossed to Landsberg *erecta*. The F1 progeny were allowed to self-fertilize, and in the F2 generation cosegregation of the photorespiratory (chlorotic at ambient CO_2) phenotype with molecular markers was determined as described (Lukowitz et al., 2000; Jander et al., 2002).

Assays of Enzyme Activity

Crude extracts for measuring SHMT activity were prepared by grinding 400 mg fresh leaf tissue at 4°C in 300 μL of extraction buffer (50 mM phosphate buffer, pH 7.5, 1 mM 2-mercaptoethanol, and 2.5 mM EDTA). Extracts for measuring Fd-GOGAT activity were prepared by grinding 2 g fresh leaves at 4°C in 1 mL of extraction buffer (50 mM HEPES, pH 7.5, 15 mM KCl, 1 mM EDTA, 1 mM DTT, and 1 mM PMSF). The extracts were cleared by centrifugation at 20,000*g* for 10 min. SHMT activity was assayed by the incorporation of radioactivity from L-[3-^{3}H] serine into 5,10-methylene-tetrahydrofolate (Geller and Kotb, 1989) as modified by Voll et al. (2006). Fd-GOGAT activity was determined spectrophotometrically by following the glutamine-dependent oxidation of NADPH at 340 nm (Meers et al., 1970; Misra and Oaks, 1986). The reaction mixture contained 50 mM HEPES buffer, pH 8.5, 1% (v/v) 2-mercaptoethanol, 3.65 mM glutamine, 3 mM 2-oxoglutarate, 0.2 mM NADPH, 4 μM ferredoxin, and 0.2 mL plant extract in a final volume of 1 mL.

Plasmid Construction

To generate full-length cDNA clones, RNA was extracted from leaves of Col-0 and the *glu1-201* mutant using the RNeasy Plant Mini Kit (Qiagen). Amplification of *GLU1* and *glu1-201* cDNAs was performed using high-fidelity *Taq* polymerase (Promega) in three separate fragments with specific primers. We exploited restriction sites in the genomic sequence.

The primers GOGAT start (5′-ATGGCGATGCAATCTCTTT-3′) and Rev1*Xho*I (5′-TACCAAATGGACGAATTT-3′) were used to amplify an 1120-bp fragment including the *Xho*I site at the position 1055. The second fragment between the *Xho*I and *Bam*HI restriction sites was amplified using For1*Xho*I (5′-GAGGTTTCTTGGACATAACG-3′) and Rev2*Bam*HI (5′-GTAGTGTTGGTGAATATCCA-3′). The third fragment was amplified using For2*Bam*HI (5′-GGAATGTCACTTGGTGCTAT-3′) and Rev3 (5′-CTAAGCCGATTGAAATGTGA-3′). PCR-amplified products were cloned in the TA-cloning system (Promega). After appropriate restriction endonuclease digestion, the three resulting fragments, *Eco*RI-*Xho*I, *Xho*I-*Bam*HI, and *Bam*HI-*Not*I were isolated from agarose gels using the Gel Extraction Kit (Qiagen) and cloned into the appropriate sites in pENTR1A (Invitrogen). All clones were completely sequenced to ensure that no mutations had been introduced.

A 10-kb fragment of *GLU1* genomic DNA, which includes 1505 bp of the promoter region, was amplified from BAC clone F21E1 using a two-step PCR reaction and TaKaRa EX Taq polymerase (PanVera). The first product was generated with the specific primers GLU1B1 (5′-AAAAAG-CAGGCTcccgatgcatgcatgtttatctt-3′) and GLU1B2 (5′-AGAAAGCTGGGT-ctgagcgatatgaagtg-3′) containing 12 nucleotides of *attB* sites (capitals) and gene-specific nucleotides (lower case). The resulting product was subjected to the second PCR step with attB adapter primers attB1 (5′-GGGGACAAGTTTGTACAAAAAAGCAGGCT-3′) and attB2 (5′-GGGGA-CCACTTTGTA CAAGAAAGCTGGGT-3′). The 10-kb fragment was cloned in pDONR207 by BP clonase (Invitrogen) and then transferred to the destination vector using LR Clonase.

To generate C-terminal fusion proteins, the *GLU1* and *SHM1* genomic sequences lacking stop codons were amplified and recombined into pDONR207 (Invitrogen) and then into pMDC110 to fuse with GFP (Curtis and Grossniklaus, 2003). This clone was sequenced to confirm that the fusions were in frame.

To generate overexpression lines, the *GLU1* gene was transferred from pENTR1A, using LR Clonase (Invitrogen), to the modified binary vector pB7WG2D (Karimi et al., 2002) in which the 1060-bp 35S promoter was replaced by an ~800-bp 35S promoter from pMDC32 (Curtis and Grossniklaus, 2003) or by the *mas* promoter from 35SpBARN (LeClere and Bartel, 2001).

The *glu1*^{204} allele, which encodes a truncated Fd-GOGAT protein lacking the catalytic region, was made by deleting ~2 kb of coding sequence between *Bgl*II and *Bam*HI restriction sites, the resulting plasmid was moved to destination vector pB7WG2D.

Site-directed mutagenesis was used to create *glu1*^{M3I}, encoding a chloroplast-targeted Fd-GOGAT, and *glu1*^{M1K}, encoding a mitochondrion-targeted Fd-GOGAT. A *GLU1* promoter fragment including the first 12 amino acids of the coding sequence and the *Hin*dIII site was PCR amplified (*Hin*dIII I M3I: 5′-GAGAAGCTTAGGAACAGGGGAAAGAGA-TTGGATCGCCAT-3′ and GLU1P *Sal*I:5′-GAGGTCGACGCGTAAATTCA-CATATT-3′) and (*Hin*dIII M1K: 5′-GAGAAGCTTAGGAACAGGGGAAA-GAGATTGCATCGCCTT-3′ and GLU1P *Sal*I) to introduce the mutations (underlined in the primers) and appropriate restriction sites and then cloned in pENTR1A:*GLU1* using the appropriate restriction enzymes.

For plant transformation, plasmids were introduced into *Agrobacterium tumefaciens* strain AGL1 and then into wild-type, *glu1-201*, or *glu1-202* mutant plants by vacuum infiltration (Clough and Bent, 1998). Transformants were selected on agar plates containing either 30 μg/mL Basta or 15 μg/mL hygromycin. Resistant seedlings were allowed to self, and T2 seeds were collected. Several lines (at least four) for each construct and genetic background were analyzed.

Protein Gel Blot Analysis

Total leaf protein was extracted from ~300 mg of ground frozen tissue mixed with 400 μL of extraction buffer containing 4 M urea, 2.5% SDS, 20% glycerol, 20 mM Tris, pH 6.8, 1 mM EDTA, 1 mM PMSF, and 0.2% Halt Protease Inhibitor (Pierce). Mitochondria and chloroplasts were isolated and purified by Percoll density gradient centrifugation (Bergman et al., 1980). Samples (20 μg protein per lane) were separated by SDS-PAGE (Laemmli, 1970) and transferred to PVDF membrane (Millipore). Membranes were blocked for 2 h at room temperature with blocking buffer (5% powdered milk, 1% PBS, pH 7.4, and 0.05% Tween 20). Membranes were incubated for at least 4 h with primary rabbit polyclonal antibodies against SHMT (Agrisera), Fd-GOGAT (Agrisera), or PSBA (Agrisera) or mouse monoclonal antibodies against α-tubulin (Sigma-Aldrich) or the β-subunit of maize (*Zea mays*) F1-ATPase (Luethy et al., 1993). Excess antibodies were removed by washing the blot twice for 15 min in 1% milk, 1× PBS, and 0.1% Tween 20 and twice for 15 min in 1% PBST. Membranes were incubated with secondary antibody, either goat anti-rabbit IgG conjugated to horseradish peroxidase (Santa Cruz Biotechnology) or goat anti-mouse IgG conjugated to horseradish peroxidase (Bio-Rad) followed by washing as described above. Signals were detected using SuperSignal West Pico Chemiluminescent Substrate (Pierce) according to the manufacturer's instructions.

Coimmunoprecipitation

Protein extracts were prepared by grinding 2 g fresh leaves at 4°C in 1 mL of lysis buffer (50 mM Tris, pH 7.5, 150 mM KCl, 1 mM EDTA, 1 mM DTT, 0.1% Triton X-100, 1 mM PMSF, and Halt Protease Inhibitor Cocktail [Pierce]) (Shao et al., 2003). Extracts were pretreated with protein A agarose suspension (Calbiochem), cleared by centrifugation, and then incubated with anti-SHMT at 4°C for 2 h. Immunocomplexes were incubated with prewashed protein A agarose for 1 h at 4°C, collected by centrifugation, washed six times with 1 mL lysis buffer, suspended in 50 μL of 1× SDS loading buffer and boiled for 5 min. Twenty-five microliters of this solution was subjected to 8% SDS-PAGE electrophoresis. Twenty-five micrograms of total Col lysate was loaded on the same gel. Immunoblots to PVDF membrane were probed with anti-Fd-GOGAT as described above.

BiFC

Full-length *GLU1* and *SHM1* cDNAs were fused in frame to the N and C termini, respectively, of YFP using vectors pSPYNE-35S/pUC-SPYNE and pSPYCE-35S/pUC-SPYCE (Walter et al., 2004). For BiFC, the fusion constructs were transfected together or singly by the polyethylene glycol method (Yoo et al., 2007) into wild-type Col protoplasts (Jamai et al., 1996). Briefly, leaves were cut into fine strips and incubated for 90 min at 28°C in 10 mL of protoplast medium containing 500 mM sorbitol, 1 mM $CaCl_2$, 10 mM MES, pH 5.5, 0.5 mM polyvinylpolypyrrolidone, 0.1% BSA, 1.5% cellulase R10 (Yakult Honsha), and 0.1% macerozyme R10 (Yakult Honsha). Protoplasts were harvested by centrifugation at 100*g* for 2 min in protoplast medium without enzymes. For fluorescence detection, excitation was at 488 nm, and the fluorescence emission signal was collected between 498 and 561 nm. To visualize mitochondria, protoplasts were stained with 40 μM MitoTracker Red (Molecular Probes) with excitation at 568 nm and emission signal collected at 579 to 687 nm.

Subcellular Localization of SHMT1 and Fd-GOGAT

Protoplasts from 2-week-old seedlings from stable transgenic lines were isolated as described (Jamai et al., 1996). Subcellular localization of the fusion proteins was determined by fluorescence microscopy as described above.

Accession Numbers

Sequence data from this article can be found in the Arabidopsis Genome Initiative or GenBank/EMBL databases under the following accession

numbers: *5-FCL* (At5g13050), *10-FDF* (At4g17360 and At5g47435), *GL1* (At3g279920), *GLN2* (At5g35630), *GLU1* (At5g04140.1), *SHM1* (At4g37930), and *SQD1* (At4g33030).

Supplemental Data

The following materials are available in the online version of this article.

Supplemental Figure 1. Phenotypic Analysis of Photorespiratory Mutants at Ambient CO_2.

Supplemental Figure 2. Genotyping of Mutants and Transgenic Complementation Lines.

Supplemental Figure 3. Phenotypic Analysis of Ability of Constructs Bearing Various *glu1* Mutations to Rescue Growth of Photorespiratory Mutants, *glu1-201* and *glu1-202*, at Ambient CO_2.

ACKNOWLEDGMENTS

We acknowledge the ABRC (Ohio State University, Columbus, OH) for seed stocks and DNA clones and SIGnAL (Salk Institute, La Jolla, CA) for providing the sequence-indexed *Arabidopsis* T-DNA insertion mutants. We thank Ann M. Lavanway and Joohyun Lee for their help with the microscopy. This work was supported by an American Society of Plant Biologists Summer Undergraduate Research Fellowship to S.H.S. and by National Science Foundation grants to C.R.M.

Received September 15, 2008; revised January 26, 2009; accepted February 3, 2009; published February 17, 2009.

REFERENCES

Bannai, H., Tamada, Y., Maruyama, O., Nakai, K., and Miyano, S. (2002). Extensive feature detection of N-terminal protein sorting signals. Bioinformatics **18:** 298–305.

Bauwe, H., and Kolukisaoglu, U. (2003). Genetic manipulation of glycine decarboxylation. J. Exp. Bot. **54:** 1523–1535.

Bergman, A., Gardeström, P., and Ericson, I. (1980). Method to obtain a chlorophyll-free preparation of intact mitochondria from spinach leaves. Plant Physiol. **66:** 442–445.

Binda, C., Bossi, R.T., Wakatsuki, S., Arzt, S., Coda, A., Curti, B., Vanoni, M.A., and Mattevi, A. (2000). Cross-talk and ammonia channeling between active centers in the unexpected domain arrangement of glutamate synthase. Structure **8:** 1299–1308.

Boldt, R., Edner, C., Kolukisaoglu, U., Hageman, M., Weckworth, W., Wienkoop, S., Morgenthal, K., and Bauwe, H. (2005). D-Glycerate 3-kinase, the last unknown enzyme in the photorespiratory cycle in Arabidopsis, belongs to a novel kinase family. Plant Cell **17:** 2413–2420.

Bourguignon, J., Neuburger, M., and Douce, R. (1988). Resolution and characterization of the glycine-cleavage reaction in pea leaf mitochondria. Biochem. J. **255:** 169–178.

Bowes, G., Ogren, W.L., and Hageman, R.H. (1971). Phosphoglycolate production catalyzed by ribulose diphosphate carboxylase. Biochem. Biophys. Res. Commun. **45:** 716–722.

Christensen, A.C., Lyznik, A., Mohammed, S., Elowsky, C.G., Elo, A., Yule, R., and Mackenzie, S.A. (2005). Dual-domain, dual-targeting organellar protein presequences in *Arabidopsis* can use non-AUG start codons. Plant Cell **17:** 2805–2816.

Clough, S.J., and Bent, A.F. (1998). Floral dip: A simplified method for *Agrobacterium*-mediated transformation of *Arabidopsis thaliana.* Plant J. **16:** 735–743.

Collakova, E., Goyer, A., Naponelli, V., Krassovskaya, I., Gregory, J.F.I., Hanson, A.D., and Shachar-Hill, Y. (2008). Arabidopsis 10-formyl tetrahydrofolate deformylases are essential for photorespiration. Plant Cell **20:** 1818–1832.

Coschigano, K.T., Melo-Oliveira, R., Lim, J., and Coruzzi, G.M. (1998). Arabidopsis *gls* mutants and distinct Fd-GOGAT genes: implications for photorespiration and primary nitrogen assimilation. Plant Cell **10:** 741–752.

Curtis, M.D., and Grossniklaus, U. (2003). A Gateway cloning vector set for high-throughput functional analysis of genes in planta. Plant Physiol. **133:** 462–469.

Douce, R., Bourguignon, J., Neuburger, M., and Rébeillé, F. (2001). The glycine decarboxylase system: A fascinating complex. Trends Plant Sci. **6:** 167–176.

Douce, R., and Neuburger, M. (1999). Biochemical dissection of photorespiration. Curr. Opin. Plant Biol. **2:** 214–222.

Droux, M., Ruffet, M.L., Douce, R., and Job, D. (1998). Interactions between serine acetyl-transferase and O-acetylserine (thiol) lyase in higher plants. Structural and kinetic properties of the free and boundzymes. Eur. J. Biochem. **255:** 235–245.

Emanuelsson, O., Nielsen, H., Brunak, S., and von Heijne, G. (2000). Predicting subcellular localization of proteins based on their N-terminal amino acid sequence. J. Mol. Biol. **300:** 1005–1016.

Eubel, H., Lee, C.P., Kuo, J., Meyer, E.H., Taylor, N.L., and Millar, A.H. (2007). Free-flow electrophoresis for purification of plant mitochondria by surface charge. Plant J. **52:** 583–594.

Geller, A.M., and Kotb, M.Y. (1989). A binding assay for serine hydroxymethyltransferase. Anal. Biochem. **180:** 120–125.

Goyer, A., Collakova, E., de la Garza, R.D., Quinlivan, E.P., Williamson, J., Gregory, J.F., Shachar-Hill, Y., and Hanson, A.D. (2005). 5-Formyltetrahydrofolate is an inhibitory but well tolerated metabolite in *Arabidopsis* leaves. J. Biol. Chem. **280:** 26137–26142.

Heazlewood, J.L., Verboom, R.E., Tonti-Filippini, J., Small, I., and Millar, A.H. (2007). SUBA: The Arabidopsis Subcellular Database. Nucleic Acids Res. **35:** D213–D218.

Jamai, A., Tommasini, R., Martinoia, E., and Delrot, S. (1996). Characterization of glutathione uptake in broad bean leaf protoplasts. Plant Physiol. **111:** 1145–1152.

Jander, G., Norris, S.R., Rounsley, S.D., Bush, D.F., Levin, I.M., and Last, R.L. (2002). Arabidopsis map-based cloning in the post-genome era. Plant Physiol. **129:** 440–450.

Karimi, M., Inzé, D., and Depicker, A. (2002). GATEWAY vectors for Agrobacterium-mediated plant transformation. Trends Plant Sci. **7:** 193–195.

Keys, A.J., Bird, I.F., Cornelius, M.J., Lea, P.J., Wallsgrove, R.M., and Miflin, B.J. (1978). Photorespiratory nitrogen cycle. Nature **275:** 741–743.

Kozaki, A., and Takeba, G. (1996). Photorespiration protects C3 plants from photooxidation. Nature **384:** 557–560.

Laemmli, U.K. (1970). Cleavage of structural proteins during the assembly of the head of bacteriophage T4. Nature **227:** 680–685.

Lea, P.J., and Miflin, B.J. (1974). An alternative route for nitrogen assimilation in higher plants. Nature **251:** 614–616.

LeClere, S., and Bartel, B. (2001). A library of Arabidopsis 35S-cDNA lines for identifying novel mutants. Plant Mol. Biol. **46:** 695–703.

Lee, D.W., Kim, J.K., Lee, S., Choi, S., Kim, S., and Hwang, I. (2008). Arabidopsis nuclear-encoded plastid transit peptides contain multiple sequence subgroups with distinctive chloroplast-targeting sequence motifs. Plant Cell **20:** 1603–1622.

Leegood, R.C., Lea, P.J., Adcock, M.D., and Häusler, R.E. (1995). The regulation and control of photorespiration. J. Exp. Bot. **46:** 1397–1414.

Linka, M., and Weber, A.P.M. (2005). Shuffling ammonia between mitochondria and plastids during photorespiration. Trends Plant Sci. **10:** 461–465.

Luethy, M.H., Horak, A., and Elthon, T.E. (1993). Monoclonal antibodies to the α- and β-subunits of the plant mitochondrial F1-ATPase. Plant Physiol. **101:** 931–937.

Lukowitz, W., Gillmor, C.S., and Scheible, W.-R. (2000). Positional cloning in Arabidopsis. Why it feels good to have a genome initiative working for you. Plant Physiol. **123:** 795–806.

Mackenzie, S.A. (2005). Plant organellar protein targeting: a traffic plan still under construction. Trends Cell Biol. **15:** 548–554.

Márquez, A.J., Avila, C., Forde, B.G., and Wallsgrove, R.M. (1988). Ferredoxin-glutamate synthase from barley leaves: Rapid purification and partial characterization. Plant Physiol. Biochem. **43:** 645–651.

McClung, C.R., Hsu, M., Painter, J.E., Gagne, J.M., Karlsberg, S.D., and Salomé, P.A. (2000). Integrated temporal regulation of the photorespiratory pathway: Circadian regulation of two Arabidopsis genes encoding serine hydroxymethyltransferase. Plant Physiol. **123:** 381–392.

Meers, J.L., Tempest, D.W., and Brown, C.M. (1970). Glutamine (amide): 2-Oxoglutarate amino transferase oxidoreductase (NADP), an enzyme involved in the synthesis of glutamate by some bacteria. J. Gen. Microbiol. **64:** 187–194.

Misra, S., and Oaks, A. (1986). Ferredoxin and pyridine nucleotide-dependent glutamate synthase activities in maize endosperm. Plant Sci. **39:** 1–5.

Murashige, T.R., and Skoog, F. (1962). A revised medium for rapid growth and bioassays with tobacco tissue culture. Physiol. Plant. **15:** 473–497.

Ogren, W.L., and Bowes, G. (1971). Ribulose diphosphate carboxylase regulates soybean photorespiration. Nat. New Biol. **230:** 159–160.

Pajuelo, P., Pajuelo, E., Forde, B.G., and Márquez, A.J. (1997). Regulation of the expression of ferredoxin-glutamate synthase in barley. Planta **203:** 517–525.

Reumann, S., and Weber, A.P.M. (2006). Plant peroxisomes respire in the light: Some gaps of the photorespiratory C2 cycle have become filled—Others remain. Biochim. Biophys. Acta **1763:** 1496–1510.

Richter, U., Kiessling, J., Hedtke, B., Decker, E., Reski, R., Börner, T., and Weihe, A. (2002). Two *RpoT* genes of *Physcomitrella patens* encode phage-type RNA polymerases with dual targeting to mitochondria and plastids. Gene **290:** 95–105.

Roje, S., Janave, M.T., Ziemak, M.J., and Hanson, A.D. (2002). Cloning and characterization of mitochondrial 5-formyltetrahydrofolate cycloligase from higher plants. J. Biol. Chem. **277:** 42748–42754.

Ruffet, M.L., Droux, M., and Douce, R. (1994). Purification and kinetic properties of serine acetyltransferase free of O-acetyl-serine(thiol) lyase from spinach chloroplasts. Plant Physiol. **104:** 597–604.

Shao, F., Golstein, C., Ade, J., Stoutemyer, M., Dixon, J.E., and Innes, R.W. (2003). Cleavage of Arabidopsis PBS1 by a bacterial type III effector. Science **301:** 1230–1233.

Shimojima, M., Hoffmann-Benning, S., Garavito, R.M., and Benning, C. (2005). Ferredoxin-dependent glutamate synthase moonlights in plant sulfolipid biosynthesis by forming a complex with SQD1. Arch. Biochem. Biophys. **436:** 206–214.

Silva-Filho, M.C. (2003). One ticket for multiple destinations: Dual targeting of proteins to distinct subcellular locations. Curr. Opin. Plant Biol. **6:** 589–595.

Small, I., and Peeters, N. (2001). Dual targeting to mitochondria and chloroplasts. Biochim. Biophys. Acta **1541:** 54–63.

Somerville, C.R. (1986). Analysis of photosynthesis with mutants of higher plants and algae. Annu. Rev. Plant Physiol. **37:** 467–507.

Somerville, C.R. (2001). An early Arabidopsis demonstration. Resolving a few issues concerning photorespiration. Plant Physiol. **125:** 20–24.

Somerville, C.R., and Ogren, W.L. (1980). Inhibition of photosynthesis in *Arabidopsis* mutants lacking leaf glutamate synthase activity. Nature **286:** 257–259.

Somerville, C.R., and Ogren, W.L. (1981). Photorespiration-deficient mutants of *Arabidopsis thaliana* lacking mitochondrial serine transhydroxymethylase activity. Plant Physiol. **67:** 666–671.

Stover, P., and Schirch, V. (1993). The metabolic role of leucovorin. Trends Biochem. Sci. **18:** 102–106.

Suzuki, A., and Rothstein, S. (1997). Structure and regulation of ferredoxin-dependent glutamate synthase from *Arabidopsis thaliana*: Cloning of cDNA, expression in different tissues of wild-type and *gltS* mutant strains, and light induction. Eur. J. Biochem. **243:** 708–718.

Taira, M., Valtersson, U., Burkhardt, B., and Ludwig, R.A. (2005). *Arabidopsis thaliana GLN2*-encoded glutamine synthetase is dual targeted to leaf mitochondria and chloroplasts. Plant Cell **16:** 2048–2058.

Timm, S., Nunes-Nesi, A., Parnik, T., Morgenthal, K., Wienkoop, S., Keerberg, O., Weckwerth, W., Kleczkowski, L.A., Fernie, A.R., and Bauwe, H. (2008). A cytosolic pathway for the conversion of hydroxypyruvate to glycerate during photorespiration in Arabidopsis. Plant Cell **20:** 2848–2859.

Turner, S.R., Ireland, R., Morgan, C., and Rawsthorne, S. (1992). Identification and localization of multiple forms of serine hydroxymethyltransferase in pea (*Pisum sativum*) and characterization of a cDNA encoding a mitochondrial isoform. J. Biol. Chem. **267:** 13528–13534.

van den Heuvel, R.H.H., Ferrari, D., Bossi, R.T., Ravasio, S., Curti, B., Vanoni, M.A., Florencio, F.J., and Mattevi, A. (2002). Structural studies on the synchronization of catalytic centers in glutamate synthase. J. Biol. Chem. **277:** 24579–24583.

Voll, L.M., Jamai, A., Renné, P., Voll, H., McClung, C.R., and Weber, A.P.M. (2006). The photorespiratory *Arabidopsis thaliana shm1* mutant is deficient in *SHM1.* Plant Physiol. **140:** 59–66.

Walter, M., Chaban, C., Schütze, K., Batistic, O., Weckermann, K., Näke, C., Blazevic, D., Grefen, C., Schumacher, K., Oecking, C., Harter, K., and Kudla, J. (2004). Visualization of protein interactions in living plant cells using bimolecular fluorescence complementation. Plant J. **40:** 428–438.

Weber, A.P.M. (2004). Solute transporters as connecting elements between cytosol and plastid stroma. Curr. Opin. Plant Biol. **7:** 247–253.

Wingler, A., Lea, P.J., Quick, W.P., and Leegood, R.C. (2000). Photorespiration: Metabolic pathways and their role in stress protection. Philos. Trans. R. Soc. Lond. B Biol. Sci. **355:** 1517–1529.

Winkel, B.S.J. (2004). Metabolic channeling in plants. Annu. Rev. Plant Biol. **55:** 85–107.

Yoo, S.-D., Cho, Y.-H., and Sheen, J. (2007). Arabidopsis mesophyll protoplasts: A versatile cell system for transient gene expression analysis. Nat. Protocols **2:** 1565–1572.

Zhu, X.-G., Long, S.P., and Ort, D.R. (2008). What is the maximum efficiency with which photosynthesis can convert solar energy into biomass? Curr. Opin. Biotechnol. **19:** 153–159.

Zischka, H., Braun, R.J., Marantidis, E.P., Buringer, D., Bornhovd, C., Hauck, S.M., Demmer, O., Gloeckner, C.J., Reichert, A.S., Madeo, F., and Ueffing, M. (2006). Differential analysis of *Saccharomyces cerevisiae* mitochondria by free flow electrophoresis. Mol. Cell. Proteomics **5:** 2185–2200.